Evidence of a direct influence between the thalamus and hMT+ independent of V1 in the human brain as measured by fMRI

Anna Gaglianese [a], Mauro Costagli [b,c], Giulio Bernardi [a], Emiliano Ricciardi [a,d,*], Pietro Pietrini [a]

[a] Laboratory of Clinical Biochemistry and Molecular Biology, University of Pisa Medical School, Pisa, Italy
[b] Fondazione IMAGO7, Calambrone, Pisa, Italy
[c] Laboratory for Cognitive Brain Mapping, RIKEN Brain Science Institute, Wako, Japan
[d] Fondazione G. Monasterio CNR-Regione Toscana, Pisa, Italy

ARTICLE INFO

ABSTRACT

In the present study we employed Conditional Granger Causality (CGC) and Coherence analysis to investigate whether visual motion-related information reaches the human middle temporal complex (hMT+) directly from the Lateral Geniculate Nucleus (LGN) of the thalamus, by-passing the primary visual cortex (V1). Ten healthy human volunteers underwent brain scan examinations by functional magnetic resonance imaging (fMRI) during two optic flow experiments.

In addition to the classical LGN-V1-hMT+ pathway, our results showed a significant direct influence of the blood oxygenation level dependent (BOLD) signal recorded in LGN over that in hMT+, not mediated by V1 activity, which strongly supports the existence of a bilateral pathway that connects LGN directly to hMT+ and serves visual motion processing. Furthermore, we evaluated the relative latencies among areas functionally connected in the processing of visual motion. Using LGN as a reference region, hMT+ exhibited a statistically significant earlier peak of activation as compared to V1.

In conclusion, our findings suggest the co-existence of an alternative route that directly links LGN to hMT+, bypassing V1. This direct pathway may play a significant functional role for the faster detection of motion and may contribute to explain persistence of unconscious motion detection in individuals with severe destruction of primary visual cortex (blindsight).

© 2012 Elsevier Inc. All rights reserved.

Introduction

The middle temporal area (MT) is a region of the extrastriate cortex first described in non-human primates (Allman and Kaas, 1971; Dubner and Zeki, 1971), whose presumable human homologue was identified as a part of the human middle temporal complex (hMT+) (Amano et al., 2009; DeYoe et al., 1996; Dukelow et al., 2001; Dumoulin et al., 2000; Huk and Heeger, 2001; Tootell et al., 1995). This cortical region plays a fundamental role in visual motion perception, and comprises a series of neighboring yet functionally segregated areas (Kolster et al., 2010). The major pathway conveying visual motion information from the retina to MT involves two main processing stages, one at the level of the thalamus, in the Lateral Geniculate Nucleus (LGN), and the other one in the primary visual cortex (V1) (Born and Bradley, 2005).

In addition, anatomical studies in primates have suggested the existence of at least two other retinothalamic pathways that convey visual motion information from the thalamus straight to area MT, that is, without passing through V1. The first one includes direct projections from the koniocellular layers of the LGN (Sincich et al., 2004; Warner et al., 2010), while the other one gathers projections from the inferior pulvinar nucleus (PUL) (Adams et al., 2000; Berman and Wurtz, 2008, 2010; Lin and Kaas, 1980; Nassi and Callaway, 2006; Stepniewska et al., 1999). Additional pieces of evidence in support of these direct anatomical connections in humans come from the results of Diffusion Tensor Imaging (DTI) and tractography studies (Bridge et al., 2008; Lanyon et al., 2009).

Although this anatomical link is less prominent than the well-established connection through V1, its existence raises the question of which functional role this connection may play. Studies in non-human primates reported that the inactivation of V1 is not associated with a complete silencing of MT neuronal populations (Girard et al., 1992; Rodman et al., 1989, 1990; Rosa et al., 2000; Schmid et al., 2010), suggesting that at least part of the visual motion information is carried to this region through alternative pathways that do not necessarily involve V1.

In humans, findings in line with the data above have been observed in the case of specific pathologies, such as blindsight, in which patients with a complete destruction of primary visual cortex

---

display some residual ability to discriminate certain visual features (e.g., motion, but also color) in the absence of conscious visual perception (Barbur et al., 1993; Schoenfeld et al., 2002; Zeki, 1995; Zeki and Ffytche, 1998). Furthermore, neural activity in MT may precede that in V1 in response to moving visual stimulation (Lamme and Roelfsema, 2000), both in monkeys (Raiguel et al., 1989, 1999) and humans (Buchner et al., 1997; Ffytche et al., 1995). Finally, reduced perception of motion in humans as a consequence of the transient disruption of hMT+ activity by transcranial magnetic stimulation (TMS) applied at or near motion onset demonstrated that an important portion of visual information reaches hMT+ earlier than it would be expected if the flow of information passed exclusively through the pathway including V1 (Beckers and Zeki, 1995; Laycock et al., 2007).

While all these findings may suggest a direct link from the thalamus to hMT+, a direct functional influence exerted by thalamic nuclei on hMT+ remains to be proven. Thus, the aim of the present study was to measure a direct influence of the thalamus over hMT+, independent of V1 activity, in the healthy human brain during visual motion perception.

To pursue this aim, we conducted functional Magnetic Resonance Imaging (fMRI) experiments to record brain activity in response to moving visual stimuli. Effective connectivity among the areas functionally connected in the processing of visual motion was explored by Conditional Granger Causality (Chen et al., 2006; Gao et al., 2011), and focused on the connections within a cortical network that comprises two thalamic nuclei, namely the LGN and the PUL, and the cortical areas V1 and hMT+.

We questioned also which functional role a direct connection between the thalamus and hMT+ may subserve. That this direct pathway may function as a 'back-up' circuit to maintain some visual information flow to hMT+ in the case of a major damage to primary visual cortical areas, as suggested by clinical studies in patients with blindsight, does not explain its functional role under physiological conditions nor can it by itself account for the selection of such an alternative pathway during evolution. On the basis of relative BOLD latencies among thalamic nuclei, V1 and hMT+, computed via Coherence analysis (Lauritzen et al., 2009; Sun, 2004; Sun et al., 2005), we speculate that this direct link may subserve a faster processing of visual motion, allowing for a pre-conscious perception of (and response to) rapidly moving stimuli.

Materials and methods

Brain activity from a total of ten healthy human volunteers with normal or corrected-to-normal vision was recorded by fMRI, during two distinct visual experiments designed to induce a neural response in the thalamo-cortical network involved in visual motion processing. All subjects underwent medical, neurological and psychiatric evaluation to rule out conditions that could affect brain function or metabolism. No subject had been taking any medication for at least two weeks before the study. All participants gave their written informed consent to participate in the study. The study was approved by the Ethical Committee of the University of Pisa.

Data were acquired on a GE Signa 1.5 Tesla scanner (General Electric, Milwaukee, WI). At the beginning of each experimental session, whole-brain T1-weighted SPGR images at a resolution of 1 mm (isotropic) were acquired for each subject. In the functional experiments, a field of view (FOV) of $240 \times 240 \times 39$ mm was imaged by 13 axial slices (matrix size: 128×128), resulting in a resolution of $1.875 \times 1.875 \times 3$ mm, and covered V1, hMT+ and the thalamic nuclei PUL and LGN of both hemispheres. Functional images were acquired every 1500 ms. Echo time and flip angle were set to 40 ms and 90°, respectively.

Visual stimuli consisted of patterns of either moving or static small white dots on a black background (dot density: 4 dots/cm^2, dot radius: 0.034°). In both experimental paradigms, the static dots corresponded to the last frame of the moving dot stimuli so that all the visual parameters (including luminance, contrast, number of stimuli, dot density and radius, etc.) were exactly identical across the two experimental conditions. Stimuli were presented to subjects in the MRI scanner by the means of a setup consisting of a projector, a screen, and a two-mirror system, as described in Ricciardi et al. (2007) and Sani et al. (2010). In both the experiments, subjects were instructed to fixate a cross at the center of the screen.

Experiment 1 — block design

Four healthy volunteers (2 females, 26 ± 1 years old) participated in this experiment. Subjects underwent two identical runs in which they were presented with visual stimuli in a block design paradigm. Each block consisted of dots moving radially outward at a speed of 6.8°/s for 9 s, followed by a pattern of static dots displayed for 27 s. The visual angle subtended by the stimulus was 6.9°. Each cycle of moving/stationary dots was repeated seven times in each of the two runs.

Experiment 2 — event related design

Six healthy volunteers (2 females, 26 ± 3 years old) participated in this experiment, which was included to overcome potential limitations intrinsic to the block design paradigm (e.g., adaptation to experimental design and timing). One subject was excluded from the analysis because of excessive head motion. Stimuli were presented in two identical runs in an event-related fashion, in which events consisted of dots moving radially for 3 s, and were separated from each other by an inter-stimulus interval (ISI) displaying static dot patterns in a range from 6 to 12 s. As the length of ISI was randomly varied according to an exponential distribution, the event was presented to each subject from 34 to 37 times in each of the two runs. The visual angle subtended by the stimulus was increased to 9°, and the dot speed was set to 10°/s.

Preprocessing and data analysis

Data were pre-processed by using AFNI (http://afni.nimh.nih.gov/afni, Cox 1996). All datasets underwent rigid-body motion correction, slice scan time correction, spatial smoothing (3D Gaussian filter, 6-mm full-width at half-maximum), temporal linear detrending, and alignment of functional and anatomical data. Data were converted into standard Talairach coordinates (Talairach and Tournoux, 1988) and resampled to a resolution of 1 mm^3 isotropic. For each voxel of each subject, the timecourses of two runs of the same type were concatenated and processed by following a deconvolution approach (Gardner et al., 2005) using the software package mrTools (http://gru.brain.riken.jp). This type of analysis is not based on any prior assumption on the shape of the hemodynamic response function (HRF), except for its length, which we set to 25 s, similarly to other studies (Gardner et al., 2008; Wan et al., 2011). The output of this analysis is a reconstructed HRF for each voxel, as well as a measure (r^2) of stimulus-dependent BOLD activity. The significance of the BOLD activity in each voxel was assessed on the basis of statistics of the r^2 values and converted into p-values, by a bootstrapping approach (Gardner et al., 2005).

Timecourses representing the activity in LGN, PUL and V1 were extracted as follows: for each region and each hemisphere, we first identified the voxel with highest r^2 located within a maximum distance of 3 mm from the center of mass of these regions as defined in Talairach coordinates. Then, the timecourses of voxels falling inside the $3 \times 3 \times 3$ mm^3 cube centered at this location were averaged to generate the resultant time series of that ROI. The resultant timecourse of hMT+ was defined in each hemisphere by identifying the

center of mass of the cluster of activated voxels on the activation map (p<0.01) in the vicinity of well-established anatomical landmarks that define this area (Annese, 2004; Dumoulin et al., 2000; Malikovic et al., 2006), and then averaging the timecourses of voxels falling inside the $3 \times 3 \times 3$ mm^3 cube centered at the local maxima within 3 mm of this location. Finally, a dummy ROI covering area BA43 (identified in Talairach coordinates) was used as a control region. By following the criteria above, we observed that the reconstructed HRFs in V1 in one subject were negative and, since this behavior is believed to reflect phenomena that are weakly coupled with neural activity (Schmuel et al., 2002), data from that subject were discarded.

We performed Conditional Granger Causality (CGC) and BOLD latencies measures (Coherence analysis) on the entire averaged time series of each ROI to examine the causal interactions within the selected network. Both CGC and Coherence analysis were implemented in MATLAB (The Mathworks, Natick, MA, USA).

In order to verify whether the causality between LGN and hMT+ is specific for the visual motion condition only, we performed supplementary CGC analyses. Specifically, from each run of the block design data from Experiment 1 (four subjects) we extracted and concatenated the segments of the timecourses corresponding to the static stimuli. In order to prevent that hemodynamic responses potentially related to motion stimuli were included, we used only the last 18 s (12 volumes) of the 27-second interval displaying static dots. CGC analysis was conducted on these concatenated timeseries representing the BOLD signal in response to static stimuli (total length 252 s). The same analysis was conducted also on concatenated series of the same time length, which contained the BOLD responses to the moving stimulus (each 18 second portion consisted of the 9 s corresponding to the stimulus and 9 s corresponding to the initial part of the "static" block).

Granger Causality

Granger Causality is based on the concept of predictability to determine whether a relationship of cause–effect exists between distinct time series (Geweke, 1982). Since a standard approach based on Bivariate Granger Causality (BGC) (Geweke, 1982; Goebel et al., 2003; Roebroeck et al., 2005) is not suitable to ascertain whether the flow of information between two ROIs may be mediated by a third area, we employed Conditional Granger Causality (CGC) analysis. CGC makes it possible to evaluate the causality between two ROIs, taking into account the potential influence of the remaining nodes of the network (Chen et al., 2006; Ding et al., 2006; Geweke, 1984). Conditional Granger Causality was implemented as reported in Chen et al. (2006) and Ding et al. (2006).

The optimal order of the autoregressive model describing the interacting time-series was either one or two, depending on the hemispheres, as determined by the Schwartz criterion (Roebroeck et al., 2005). The coefficients of CGC $F_{y->x|z}(f)$ were computed on the averaged time series of the ROIs every 0.01 Hz in the frequency range 0.01–0.12 Hz, which encompasses the relevant frequencies of the typical hemodynamic response functions that characterize the BOLD-fMRI signal (Cordes et al., 2001; Lauritzen et al., 2009; Sun, 2004). To infer the significance of the CGC coefficients of each pairwise combination of ROIs, a bootstrap distribution of size 1000 was computed for each frequency by shuffling the estimated autoregressive coefficients that describe the data. The significance of a CGC coefficient $F_{y->x|z}(f)$ was assessed by computing, for each frequency, the percentage of bootstrapped coefficients that were smaller than the real one (Gardner et al., 2005; Havlicek et al., 2010). A connection was considered significant if at least one CGC coefficient passed the 95th percentile threshold, meaning that at least 950 out of 1000 bootstrapped coefficients were smaller than the real one. A single value representing the significance of each connection, for each subject, was computed as the sum of the significant GC coefficients in the frequency band, divided by the total number of the bands.

BOLD response latencies measured by Coherence analysis

Cross-spectral densities, hence coherence $Coh_{xy}(f)$ and phase values $\phi_{xy}(f)$ as defined in Sun et al. (2005), were estimated in MATLAB by Welch's periodogram-averaging method in 12 frequency bands as in the GC analysis, for each combination of ROIs that resulted significant in the CGC analysis, by calculating the discrete Fourier transform in 64 points and employing a Hanning window with 50% overlap (Sun, 2004). Connections of interest that resulted significant in the CGC analysis were characterized in terms of latency L_{xy}, defined as the mean of $\phi_{xy}(f_i)/2\pi f_i$, where f_i are the frequencies each band was centered at.

Results

Task-related brain activation maps

During both visual motion experiments, subjects consistently exhibited neural activation responses in hMT+ and in areas within the early visual cortex. Statistical r^2 maps (p<0.05) and reconstructed HRF for V1 and hMT+ for a representative subject who participated in the block design experiment are reported in Fig. 1a. Our protocol successfully elicited significant BOLD responses in the LGN as well, in 14 out of 18 hemispheres, as shown in the example in Fig. 1b, which illustrates activated LGN voxels in the same subject (p<0.05).
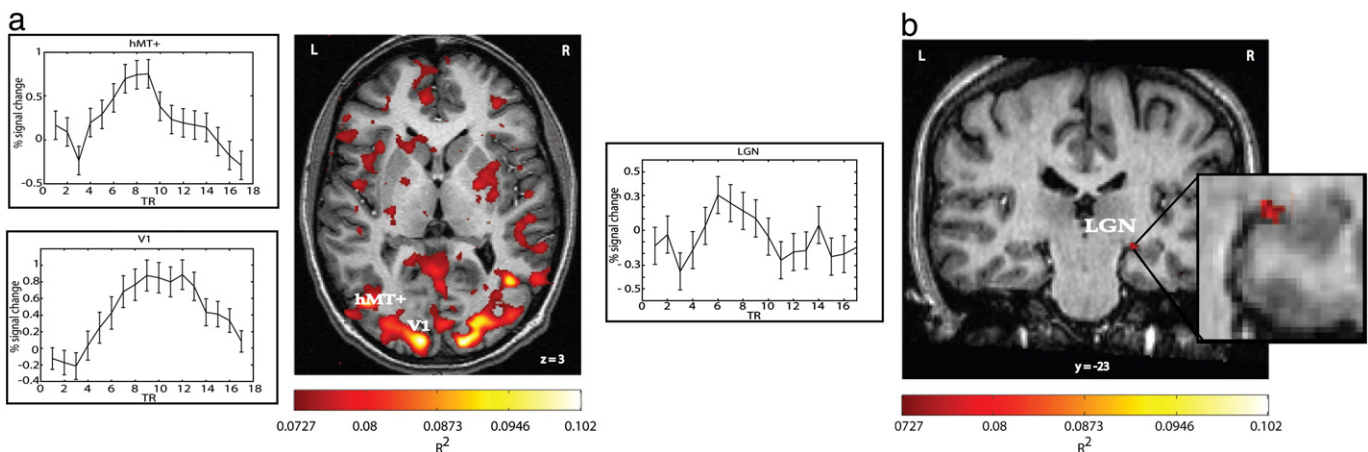
Fig. 1. Statistical activation maps (p<0.05) for one representative subject: statistical activation maps and reconstructed HRF (mean and standard error) for hMT+ and V1 (a) and LGN activated voxels (b).

Table 1
Mean and standard deviation of the Talairach coordinates of the local maxima of each selected ROI.

Regions	Right			Left		
	X	Y	Z	X	Y	Z
LGN	22 ± 2.59	-22 ± 2.35	-1 ± 2.78	-22 ± 1.8	-25 ± 2.68	-1 ± 2.39
PUL	15 ± 2.28	-26 ± 2.17	8 ± 2.59	-17 ± 1.67	-26 ± 1.99	8 ± 2.44
V1	12 ± 1.66	-88 ± 2.55	4 ± 2.16	-11 ± 1.94	-89 ± 2.55	5 ± 2.37
hMT+	44 ± 3.10	-63 ± 5.17	2 ± 4.87	-41 ± 3.54	-67 ± 3.90	2 ± 3.39

On the other hand, the PUL was significantly activated only in 7 out of 18 hemispheres. The means and standard deviations of the Talairach coordinates of the centers of the corresponding ROIs for the right and left hemispheres, respectively, are presented in Table 1.

Effective connectivity as measured by CGC analysis

Analysis of the fMRI BOLD data for both experiments by CGC demonstrated the existence of a significant effective connectivity from LGN to hMT+ that was not mediated by V1.

Fig. 2a illustrates the CGC coefficients for the connection from LGN to hMT+, calculated for one representative hemisphere in the frequency range of interest. The null distribution of the corresponding coefficients is shown in terms of mean and standard deviation, as well. To assess the significance of the connection, each estimated coefficient computed from the actual data was compared to those of the null distribution. For each frequency, the number of bootstrapped CGC coefficients that were smaller than the measured one is displayed in Fig. 2b. CGC coefficients were assumed to be significant when they were greater than the 95th percentile of the bootstrapped ones (see Materials and methods). For example, the coefficient computed from the real data in the frequency band centered at 0.09 Hz was greater than 995 out of 1000 bootstrapped coefficients, as shown in detail in Fig. 3, meaning that the connection in this frequency band held an estimated significance $p < 0.005$. All bands centered between 0.01 and 0.12 Hz held an estimated significance $p < 0.05$ (Fig. 2b).

For comparison, connectivity coefficients obtained by standard BGC analysis between the same two ROIs are reported in Fig. 4. Compared to CGC analysis, BGC held greater though less significant coefficients because they represent not only the direct flow of information leaving LGN and reaching hMT+, but also the spurious influence of LGN on hMT+ that is mediated by V1.
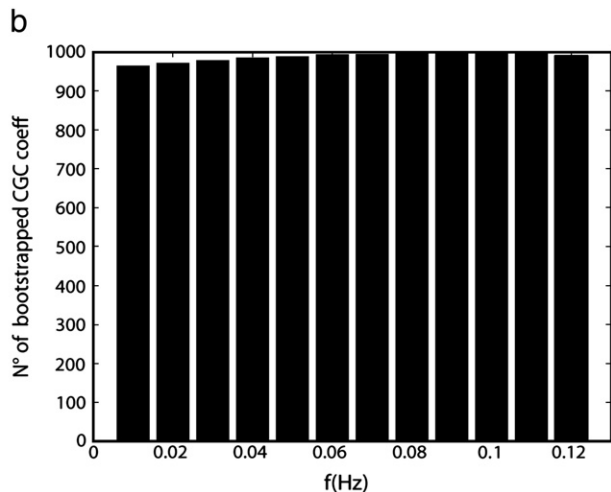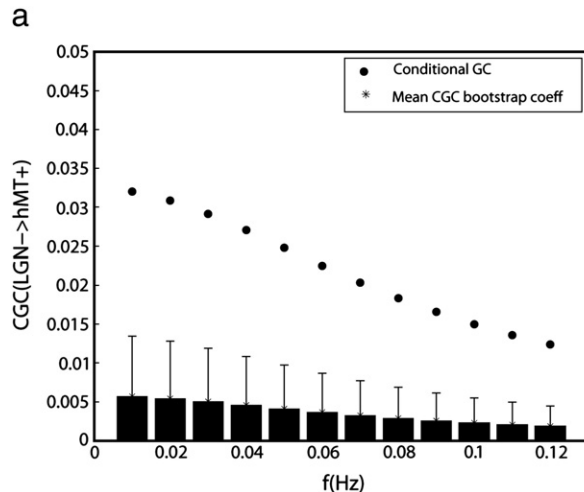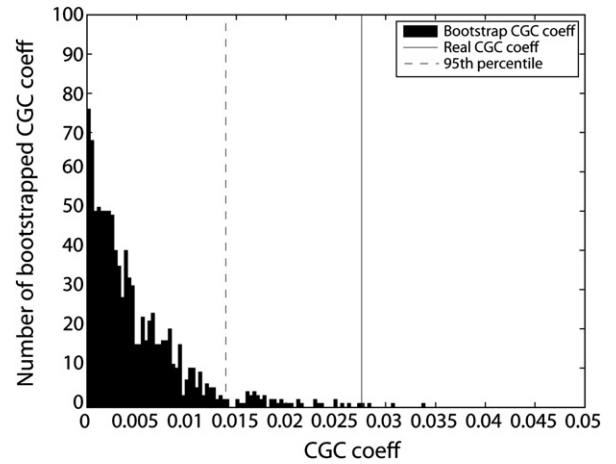
Fig. 3. CGC result for the connection LGN➔hMT+|V1,PUL for f = 0.09 Hz: distribution of the CGC coefficients obtained by bootstrap procedure for the frequency band centered at 0.09 Hz for one representative hemisphere. Dashed line represents the 95th percentile of the bootstrapped distribution, and solid line shows the CGC coefficient obtained with actual data.

Overall, seven out of eight subjects exhibited significant CGC coefficients in at least one hemisphere, proving that information flows from LGN directly to hMT+, bypassing V1. In particular, five subjects exhibited bilateral direct connectivity, while two subjects displayed this property only in one hemisphere (one right hemisphere and one left hemisphere; see Table 2, first column, for details).

The direct flow of information in the opposite direction (namely, hMT+➔LGN|V1, PUL) was found to be significant only in a single hemisphere of three subjects. The connection of the PUL with hMT+ was significant only in three subjects, monolaterally, for the PUL➔hMT+|LGN, V1 direction, while it was significant in five out of eight subjects in the opposite direction.

CGC analysis was performed also to assess the other possible connections within the network comprising LGN, PUL, V1 and hMT+. Each direct connection between two nodes was evaluated after excluding the influence of the other two nodes of the network to control for effects of spurious connectivity. Results are reported in Table 2.

The most prominent direct connection was V1➔hMT+, which was detected in seven out of eight subjects, in 14 out 16 hemispheres (seven of the right hemispheres and seven of the left ones). The coefficients representing strength of this direct connection were the largest, compared to the coefficients obtained for any other connection

Fig. 2. CGC results: a) CGC coefficients (black circles) and bootstrapped distributions (bars, mean and standard deviation) for the connection LGN→hMT+|V1, PUL in one representative hemisphere. b) Number of bootstrapped CGC coefficients that are smaller than the actual one for each frequency band.
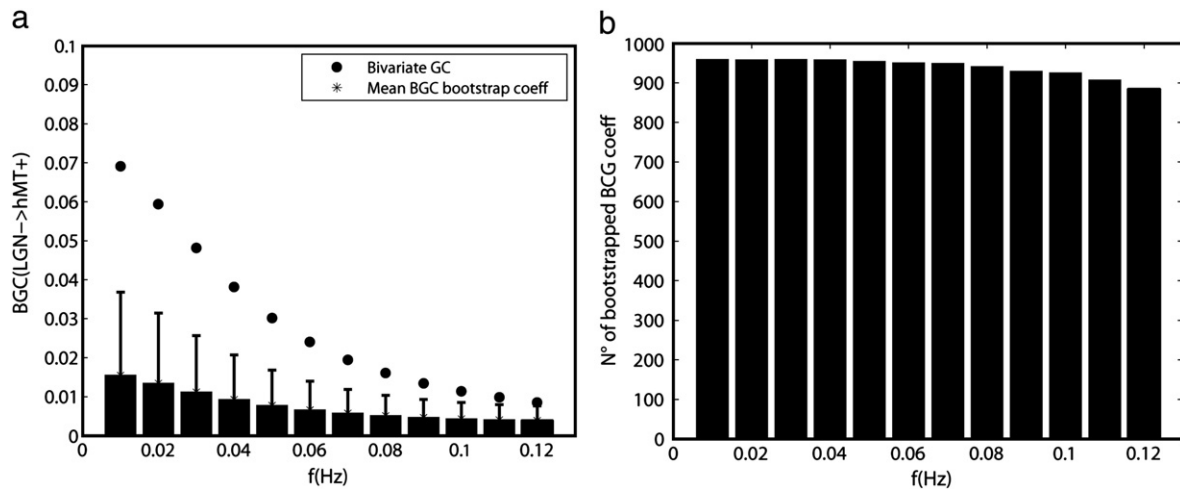
Fig. 4. BGC results: a) BGC coefficients (black circles) and bootstrapped distributions (bars, mean and standard deviation) for the connection LGN→hMT+ in one representative hemisphere. b) Number of bootstrapped BGC coefficients that are smaller than the actual one for each frequency band.

that was analyzed. The feedback connection in the opposite direction was detected in seven subjects, as well.

A summary of our results is presented in Fig. 5, in which CGC coefficients for each connection averaged across subjects and the number of significant hemispheres are reported.

Furthermore, to test specificity of the findings, Granger Causality was calculated also between LGN and a dummy ROI in a region that was not expected to receive any significant flow of information following a visual motion stimulus, namely Brodmann area 43 (BA43), which is part of the gustatory pathway (Small et al., 1999). The analysis for this connection provided one significant coefficient in only one out of 16 hemispheres, indicating no functional connection with brain areas that are not known for being involved in visual processing.

Finally, we verified the specificity of the LGN➔hMT+ causality in response to moving stimuli by performing CGC between these two regions (specifically LGN➔hMT+|V1, PUL) for both concatenated time series including moving dot stimuli and static dot stimuli, respectively, on the block design data from Experiment 1. Results for the concatenated time series representing the responses to static stimuli showed that seven out of eight hemispheres displayed no significant causality between LGN and hMT+, while in the case of the concatenated time series including moving stimuli six out of eight hemispheres displayed significant results demonstrating that the alternative pathway connecting directly the LGN to hMT+ exhibits a strong preference for moving stimuli. These findings replicate the results of the main effective connectivity analysis measured on the entire time series by indicating that the causality between LGN and hMT+ is due to the processing of visual motion and not merely to the perception of static stimuli.

BOLD response latencies measured by Coherence analysis

The BOLD latencies between LGN and hMT+ and between LGN and V1 were analyzed in terms of phase delay, as well, in those hemispheres where CGC results were significant for both connections (7 subjects; one left and six right hemispheres). The median phase delay characterizing the connection LGN-hMT+ was 0.254 s (standard error = 0.16 s), which means that activity in hMT+ follows activity in LGN by a few hundred milliseconds (Fig. 6, bar on the left). We performed the same measurement for the connection LGN-V1 and we computed the difference between the phase delays of the connections LGN-hMT+ and LGN-V1 in each hemisphere. These differences were statistically significant (one-sided *t*-test, p = 0.0019) with a median of −0.544 s (standard error = ±0.13 s) (Fig. 6, bar

on the right), indicating that the visual motion stimuli elicited brain responses whose hemodynamics appeared first in LGN, then in hMT+, and at last in V1.

Coherence analysis on the PUL-hMT+ connection was not performed given that only three out of eight subjects exhibited significant CGC coefficients.

Discussion

Our results showed that neural activity, as measured by the BOLD signal, in LGN directly influences activity in hMT+, independently from V1, in the human brain. In fact, when the potential contribution of V1 was removed by using CGC analysis, the direct influence of the thalamic nuclei over hMT+ remained significant, in contrast to what would have occurred if activity in hMT+ was completely mediated by the primary visual cortex.

As expected, CGC analysis identified also the classical visual network connecting the thalamus to V1 and then reaching hMT+ (Born and Bradley, 2005; Ungerleider et al., 1984) as the most prominent one. Furthermore, our data revealed also the well-established backward interactions from the cortical areas hMT+ and V1 to the thalamic nuclei described in the literature (Lamme and Roelfsema,

Table 2
CGC results.

	LGN->hMT+		V1->hMT+		LGN->V1	
	L	R	L	R	L	R
Hemispheres	6	6	7	7	3	7
Subjects		7		7		7

	hMT+->LGN		hMT+->V1		V1->LGN	
	L	R	L	R	L	R
Hemispheres	2	1	6	4	5	2
Subjects		3		7		7

	PUL->hMT+		PUL->V1		LGN->PUL	
	L	R	L	R	L	R
Hemispheres	2	1	2	3	6	6
Subjects		3		3		7

	hMT+->PUL		V1->PUL		PUL->LGN	
	L	R	L	R	L	R
Hemispheres	3	3	3	4	4	4
Subjects		5		6		6
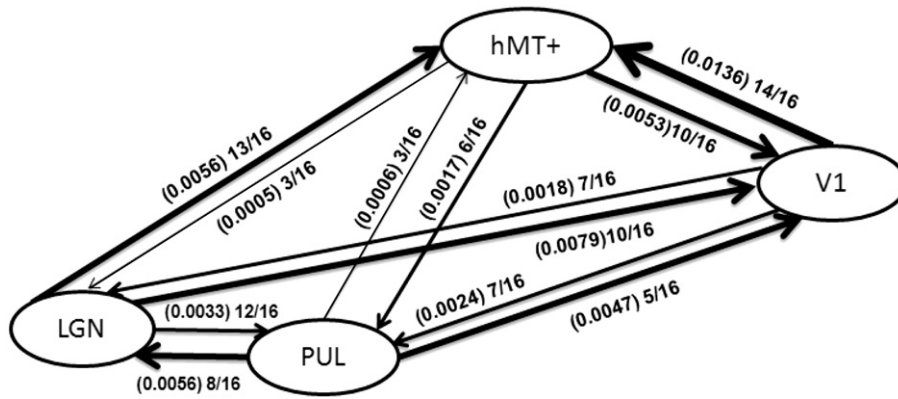
Fig. 5. CGC network: scheme representing the network of visual areas considered from a CGC standpoint. The thickness of each arrow is proportional to the mean CGC coefficients across hemispheres, as indicated by the numbers in parentheses, followed by the number of hemispheres that exhibited such connection.

2000; Sillito et al., 2006). In contrast, Granger Causality analysis did not reveal any effective connectivity between LGN and a representative region not involved in visual motion processing, namely, the gustatory area BA43.

The single-subject approach adopted in this study revealed that these functional networks were present in the majority of the examined individuals with some degree of inter-subject variability. This observation is in agreement with both functional and anatomical studies that showed a certain degree of variability across subjects in the functional recruitment of hMT+ and in the detection of anatomical connections between LGN and hMT+ (Della-Justina et al., 2007; Huk and Heeger, 2001; Lanyon et al., 2009). In contrast, the pulvinar connections were the less significant in the network since the PUL was not significantly activated in the majority of the subjects analyzed. This result is in line with the findings of Kastner et al. (2004), who explained the non-significant activation in the Pulvinar as possibly due to insufficient spatial resolution or sensitivity of the fMRI technique.

The demonstration of a direct functional influence of thalamic nuclei over hMT+ BOLD activity during visual motion perception raises the question of its physiological meaning. Electrophysiological studies in both monkeys (Raiguel et al., 1989, 1999) and humans (Buchner et al., 1997; Ffytche et al., 1995) reported that neural activity in MT+ may precede that in V1 in response to moving visual stimulation (Lamme and Roelfsema, 2000).

Taken together with our observations, one could argue that such a link may play a role in a faster processing of visual motion stimuli. To investigate this question we performed Coherence analysis to measure phase delays of the BOLD time series, among regions involved in the flow of information from the thalamus to the cortex.
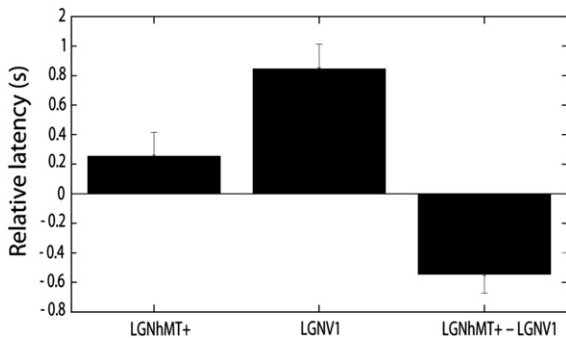
Fig. 6. Phase delays: mean phase delays in the connections LGN-hMT+ and LGN-V1 (first and second bars, respectively) and delay differences between LGN-hMT+ and LGN-V1 (third bar) computed across subjects that displayed significant connectivity in both connections. Error bars represent standard error.

Considering LGN as the reference region, results in the subjects who exhibited, for each hemisphere, significant CGC coefficients showed significantly shorter latencies in hMT+ as compared to those in V1, consistently with a faster flow of information from the thalamus to hMT+ than expected if the flow of information passed through V1.

Over the last few years, different methods have been developed to test effective connectivity between different brain areas based on the temporal dynamics of the fMRI signal. In particular, two different techniques, namely Granger Causality and Dynamic Causal Modeling (DCM), are the most widely used methods. Here, we performed CGC because this approach appeared to be the most suitable one for our experimental paradigm. First, Granger Causality analysis is a data driven exploratory approach that does not need a definite physical interpretation of its state variables since it is based on a linear stochastic autoregressive model to determine the temporal precedence between time series (Roebroeck et al., 2011). In contrast to the Dynamic Causal Modeling (Friston et al., 2003), which is a model-driven confirmatory approach based on specific hypotheses which need specification of priors and identifiability of the unknown parameters, the GC approach enables to avoid the definition of a biophysical model – which is not possible to measure in any feasible way – for each selected region of the network (Roebroeck et al., 2011). Moreover, since a number of studies stressed the importance of having spectral representation of causal influence to better capture the natural dynamics of the signals (Bressler and Seth, 2011; Ding et al., 2006; Valdes-Sosa et al., 2011), we performed CGC measures in the frequency domain.

There are, however, some cautions that must be kept in mind in applying these analyses to fMRI data (Valdes-Sosa et al., 2011). In the first place, the evaluation of the causal influence between two regions, if ignoring the potential influence of other regions involved in the network, may lead to the detection of spurious interactions (Chen et al., 2006; Ding et al., 2006; Geweke, 1984). This, though, is not the case of our results, as CGC takes into account the potential contribution of all the other nodes of the network. We are confident we considered the main brain structures primarily involved in the processing of visual motion. We included the primary visual cortex since it is the principal source of visual inputs to hMT+ and therefore it is the most likely cause of potential spurious influences of the thalamus on hMT+. However, it is well known that hMT+ possesses both forward and feedback connections with other low-order visual regions, specifically V2 and V3. Thus, in theory, these regions could receive visual inputs from V1, or less likely, directly from thalamus, and send them to hMT+, influencing its activity and determining the observation of spurious connections between LGN and hMT+ itself. However, both our Coherence analysis and consistent findings in the literature indicate that hMT+ is recruited before other lower-order visual areas (Lamme and Roelfsema, 2000; Schoenfeld et al.,

2002). Given these premises, we are confident that these regions did not influence the causal relation between LGN and hMT + that we found in the present study. Thus, the detection of significant CGC co-efficients for both directions of influence between thalamic nuclei and hMT + truly reflects the presence of a direct relationship, at least in terms of hemodynamics, between these two regions that is not mediated by V1.

One could also argue that the direction of influence reflected by the BOLD signal is strongly affected by regional differences in terms of shape and onset time of the hemodynamics. However, the variability in the hemodynamic responses across different areas within the same individual is relatively smaller than across subjects (Aguirre et al., 1997; Handwerker et al., 2004). Thus, the single subject approach that we have adopted in this study should minimize any potential variability effect. Moreover, recent studies demonstrated that, even in the presence of different hemodynamic responses, Granger Causality is able to identify the correct direction of influence between different areas with a reliable accuracy when temporal resolution is 1.5 s or less (Bressler and Seth, 2011; Deshpande et al., 2010; Schippers et al., 2011). It is important, however, to bear in mind these issues and ultimately, similarly to the case of any evidence based on the dynamics of BOLD signals, validate these results using more direct measurements of neural activity, such as magnetoencephalography or electroencephalography.

Similarly, the Coherence approach we adopted is robust in inferring BOLD delays between different areas since it does not depend on any prior assumption on the hemodynamic response function or on a definition of a biophysical model. Moreover, as shown by Lauritzen et al. (2009), and Sun (2004), the frequency-based Coherence approach that we used is not affected by interregional differences in the HRF since it measures the linear time invariant relationship between time series. The measured range of phase delay values is consistent with those reported in previous studies that have used the same methodology (Lauritzen et al., 2009; Sun et al., 2005). Indeed, the temporal precision of phase delays measures is in the range of hundreds of milliseconds due to the sluggishness of the hemodynamics, and therefore does not represent an absolute estimate of latencies in neural activity. Although this is an indirect measure of neural latency, a number of studies provided evidence for a neurovascular coupling between slow fluctuations in fMRI signals and gamma-band power in local field potentials (Leopold et al., 2003; Shmuel and Leopold, 2008), and electrophysiological studies demonstrated an earlier response component in hMT + as compared to a later peak of activity in V1 in response to moving stimuli (Buchner et al., 1997; Ffytche et al., 1995; Prieto et al., 2007).

In conclusion, our results strongly support the existence of a pathway that conveys at least part of visual information to hMT + directly from thalamic nuclei by the means of a direct, non-mediated, flow of neural information, which is possibly faster than the flow involving V1.

Moreover, our CGC analysis performed on the concatenated time-series including moving and static dot stimuli, respectively, indicates that the involvement of this connection is specific for visual motion perception, as it is absent during the perception of static stimuli.

These results support the existence of two parallel pathways: the well-established route involving V1, and an additional direct connection devoted to the processing of moving stimuli. The physiological presence of a direct connection from LGN to hMT + would be the most parsimonious explanation for the clinical observation of a relatively preserved motion perception in patients with complete or near-to-complete destructions of primary visual cortex, although one could alternatively invoke plastic functional rearrangements in the brain of these patients with blindsight (Schoenfeld et al., 2002; Zeki, 1995).

This direct link connecting thalamic nuclei and hMT + may complement the function of motion perception and pursuit accomplished by the major classical pathway that goes through V1, and may play a role for a faster and possibly preconscious perception mechanism. Such a mechanism of fast parallel processing may have played an important role in the evolution of the (human) brain, and resembles the one involved with the processing of emotions carried out by the amygdala, which is activated by the presentation of subliminal stimuli with high emotional content, even in the absence of awareness of the stimulus itself (Morris et al., 1998, 1999; Whalen et al., 1998). In the context of visual motion processing, the presence of a mechanism that is independent of (and faster than) awareness would constitute an important advantage for the detection of potentially dangerous situations at a preconscious stage. To investigate this aspect, new protocols that combine different methodological approaches and improve temporal resolution need to be developed.

Conclusion

The results of the present study indicate a direct functional connection between the thalamic nuclei and hMT + that bypasses V1. Such a direct connection may be responsible for a faster detection of movement and may contribute to explain the persistent perception of visual motion in patients with extensively damaged primary visual cortex, as well.

References

Adams, M.M., Hof, P.R., Gattass, R., Webster, M.J., Ungerleider, L.G., 2000. Visual cortical projections and chemoarchitecture of macaque monkey pulvinar. J. Comp. Neurol. 419, 377–393.

Aguirre, G.K., Zarahn, E., D'Esposito, M., 1997. The variability of human, BOLD hemodynamic responses. Neuroimage 8, 360–369.

Allman, J.M., Kaas, J.H., 1971. Representation of the visual field in striate and adjoining cortex of the owl monkey (Aotus trivirgatus). Brain Res. 35, 89–106.

Amano, K., Wandell, B.A., Dumoulin, S.O., 2009. Visual field maps, population receptive field sizes, and visual field coverage in the human MT + complex. J. Neurophysiol. 102, 2704–2718.

Annese, J., 2004. Localization of the human cortical visual area MT based on computer aided histological analysis. Cereb. Cortex 15, 1044–1053.

Barbur, J.L., Watson, J.D., Frackowiak, R.S., Zeki, S., 1993. Conscious visual perception without V1. Brain 116 (Pt 6), 1293–1302.

Beckers, G., Zeki, S., 1995. The consequences of inactivating areas V1 and V5 on visual motion perception. Brain 118 (Pt 1), 49–60.

Berman, R.A., Wurtz, R.H., 2008. Exploring the pulvinar path to visual cortex. Prog. Brain Res. 171, 467–473.

Berman, R.A., Wurtz, R.H., 2010. Functional identification of a pulvinar path from superior colliculus to cortical area MT. J. Neurosci. 30, 6342–6354.

Born, R.T., Bradley, D.C., 2005. Structure and function of visual area MT. Annu. Rev. Neurosci. 28, 157–189.

Bressler, S.L., Seth, A.K., 2011. Wiener–Granger Causality: a well established methodology. Neuroimage 58, 323–329.

Bridge, H., Thomas, O., Jbabdi, S., Cowey, A., 2008. Changes in connectivity after visual cortical brain damage underlie altered visual function. Brain 131, 1433–1444.

Buchner, H., Gobbele, R., Wagner, M., Fuchs, M., Waberski, T.D., Beckmann, R., 1997. Fast visual evoked potential input into human area V5. Neuroreport 8, 2419–2422.

Chen, Y., Bressler, S., Ding, M., 2006. Frequency decomposition of conditional Granger causality and application to multivariate neural field potential data. J. Neurosci. Methods 150, 228–237.

Cordes, D., Haughton, M., Arfanakis, K., Carew, J.D., Turski, P.A., Moritz, C.H., Quigley, M.A., Meyerand, E., 2001. Frequencies contributing to functional connectivity in the cerebral cortex in "resting-state" data. Am. J. Neuroradiol. 22, 1326–1333.

Della-Justina, H.M., Pastorello, B.F., Santos-Pontelli, T.E.G., Pontes-Neto, O.M., Santos, A.C., Baffa, O., Colafemina, J.F., Leite, J.P., Araujo, D.B., 2007. Human variability of fMRI brain activation in response to oculomotor stimuli. Brain Topogr. 20, 113–121.

Deshpande, G., Sathian, K., Hu, X., 2010. Effect of hemodynamic variability on Granger causality analysis of fMRI. Neuroimage 52, 884–896.

DeYoe, E.A., Carman, G.J., Bandettini, P., Glickman, S., Wieser, J., Cox, R., Miller, D., Neitz, J., 1996. Mapping striate and extrastriate visual areas in human cerebral cortex. Proc. Natl. Acad. Sci. U. S. A. 93, 2382–2386.

Ding, M., Chen, Y., Bressler, L.S., 2006. Granger Causality: basic theory and application to neuroscience. J. Neurosci. Methods 150, 228–237.

Dubner, R., Zeki, S.M., 1971. Response properties and receptive fields of cells in an anatomically defined region of the superior temporal sulcus in the monkey. Brain Res. 35, 528–532.

Dukelow, S.P., DeSouza, J.F., Culham, J.C., van den Berg, A.V., Menon, R.S., Vilis, T., 2001. Distinguishing subregions of the human MT+ complex using visual fields and pursuit eye movements. J. Neurophysiol. 86, 1991–2000.

Dumoulin, S.O., Bittar, R.G., Kabani, N.J., Baker Jr., C.L., Le Goualher, G., Bruce Pike, G., Evans, A.C., 2000. A new anatomical landmark for reliable identification of human area V5/MT: a quantitative analysis of sulcal patterning. Cereb. Cortex 10, 454–463.

Ffytche, D.H., Guy, C.N., Zeki, S., 1995. The parallel visual motion inputs into areas V1 and V5 of human cerebral cortex. Brain 118 (Pt 6), 1375–1394.

Friston, K.J., Harrison, L., Penny, W., 2003. Dynamic causal modelling. Neuroimage 19, 1273–1302.

Gao, Q., Duan, X., Chen, H., 2011. Evaluation of effective connectivity of motor areas during motor imagery and execution using conditional Granger causality. Neuroimage 54, 1280–1288.

Gardner, J.L., Sun, P., Waggoner, A.R., Ueno, K., Tanaka, K., Cheng, K., 2005. Contrast adaptation and representation in human early visual cortex. Neuron 47, 607–620.

Gardner, J.L., Merriam, E.P., Movshon, J.A., Heeger, D.J., 2008. Maps of visual space in human occipital cortex are retinotopic, not spatiotopic. J. Neurosci. 28, 3988–3999.

Geweke, J., 1982. Measurement of linear-dependence and feedback between multiple time-series. J. Am. Stat. Assoc. 77, 304–313.

Geweke, J.F., 1984. Measures of conditional linear-dependence and feedback between time-series. J. Am. Stat. Assoc. 79, 907–915.

Girard, P., Salin, P.A., Bullier, J., 1992. Response selectivity of neurons in area MT of the macaque monkey during reversible inactivation of area V1. J. Neurophysiol. 67, 1437–1446.

Goebel, R., Roebroeck, A., Kim, D.S., Formisano, E., 2003. Investigating directed cortical interactions in time-resolved fMRI data using vector autoregressive modeling and Granger causality mapping. Magn. Reson. Imaging 21, 1251–1261.

Handwerker, D., Ollinger, J., Desposito, M., 2004. Variation of BOLD hemodynamic responses across subjects and brain regions and their effects on statistical analyses. Neuroimage 21, 1639–1651.

Havlicek, M., Jan, J., Brazdil, M., Calhoun, V.D., 2010. Dynamic Granger causality based on Kalman filter for evaluation of functional network connectivity in fMRI data. Neuroimage 53, 65–77.

Huk, A., Heeger, D.J., 2001. Pattern-motion responses in human visual cortex. Nat. Neurosci. 5, 72–75.

Kastner, S., O'Connor, D.H., Fukui, M.M., Fehd, M.H., Herwig, U., Pinsk, M.A., 2004. Functional imaging of the human lateral geniculate nucleus and pulvinar. J. Neurophysiol. 91, 438–448.

Kolster, H., Peeters, R., Orban, G.A., 2010. The retinotopic organization of the human middle temporal area MT/V5 and its cortical neighbors. J. Neurosci. 30, 9801–9820.

Lamme, V.A., Roelfsema, P.R., 2000. The distinct modes of vision offered by feedforward and recurrent processing. Trends Neurosci. 23, 571–579.

Lanyon, L.J., Giaschi, D., Young, S.A., Fitzpatrick, K., Diao, L., Bjornson, B.H., Barton, J.J., 2009. Combined functional MRI and diffusion tensor imaging analysis of visual motion pathways. J. Neuroophthalmol. 29, 96–103.

Lauritzen, T.Z., D'Esposito, M., Heeger, D.J., Silver, M.A., 2009. Top-down flow of visual spatial attention signals from parietal to occipital cortex. J. Vis. 9 (18), 11–14.

Laycock, R., Crewther, D.P., Fitzgerald, P.B., Crewther, S.G., 2007. Evidence for fast signals and later processing in human V1/V2 and V5/MT+: a TMS study of motion perception. J. Neurophysiol. 98, 1253–1262.

Leopold, D.A., Murayama, Y., Logothesis, N.K., 2003. Very slow activity fluctuations in monkey visual cortex: implications for functional brain imaging. Cereb. Cortex 13, 422–433.

Lin, C.S., Kaas, J.H., 1980. Projections from the medial nucleus of the inferior pulvinar complex to the middle temporal area of the visual cortex. Neuroscience 5, 2219–2228.

Malikovic, A., Amunts, K., Schleicher, A., Mohlberg, H., Eickhoff, S.B., Wilms, M., Palomero-Gallagher, N., Armstrong, E., Zilles, K., 2006. Cytoarchitectonic analysis of the human extrastriate cortex in the region of V5/MT+: a probabilistic, stereotaxic map of area hOc5. Cereb. Cortex 17, 562–574.

Morris, J.S., Ohman, A., Dolan, R.J., 1998. Conscious and unconscious emotional learning in the human amygdala. Nature 393, 467–470.

Morris, J.S., Ohman, A., Dolan, R.J., 1999. A subcortical pathway to the right amygdala mediating "unseen" fear. Proc. Natl. Acad. Sci. U. S. A. 96, 1680–1685.

Nassi, J.J., Callaway, E.M., 2006. Multiple circuits relaying primate parallel visual pathways to the middle temporal area. J. Neurosci. 26, 12789–12798.

Prieto, E.A., Barnikol, U.B., Soler, E.P., Dolan, K., Hesselmann, G., Mohlberg, H., Amunts, K., Zilles, K., Niedeggen, M., Tass, P.A., 2007. Timing of V1/V2 and V5+ activations during coherent motion of dots: an MEG study. Neuroimage 37, 1384–1395.

Raiguel, S.E., Lagae, L., Gulyas, B., Orban, G.A., 1989. Response latencies of visual cells in macaque areas V1, V2 and V5. Brain Res. 493, 155–159.

Raiguel, S.E., Xiao, D.K., Marcar, V.L., Orban, G.A., 1999. Response latency of macaque area MT/V5 neurons and its relationship to stimulus parameters. J. Neurophysiol. 82, 1944–1956.

Ricciardi, E., Vanello, N., Sani, L., Gentili, C., Scilingo, E.P., Landini, L., Guazzelli, M., Bicchi, A., Haxby, J.V., Pietrini, P., 2007. The effect of visual experience on the development of functional architecture in hMT+. Cereb. Cortex 17, 2933–2939.

Rodman, H.R., Gross, C.G., Albright, T.D., 1989. Afferent basis of visual response properties in area MT of the macaque. I. Effects of striate cortex removal. J. Neurosci. 9, 2033–2050.

Rodman, H.R., Gross, C.G., Albright, T.D., 1990. Afferent basis of visual response properties in area MT of the macaque. II. Effects of superior colliculus removal. J. Neurosci. 10, 1154–1164.

Roebroeck, A., Formisano, E., Goebel, R., 2005. Mapping directed influence over the brain using Granger causality and fMRI. Neuroimage 25, 230–242.

Roebroeck, A., Formisano, E., Goebel, R., 2011. The identification of interacting networks in the brain using fMRI: model selection, causality and deconvolution. Neuroimage 58, 296–302.

Rosa, M.G., Tweedale, R., Elston, G.N., 2000. Visual responses of neurons in the middle temporal area of new world monkeys after lesions of striate cortex. J. Neurosci. 20, 5552–5563.

Sani, L., Ricciardi, E., Gentili, C., Vanello, N., Haxby, J.V., Pietrini, P., 2010. Effects of visual experience on the human MT+ functional connectivity networks: an fMRI study of motion perception in sighted and congenitally blind individuals. Front. Syst. Neurosci. 4, 159.

Schippers, M.B., Renken, R., Keysers, C., 2011. The effect of intra- and inter-subject variability of hemodynamic responses on group level Granger causality analyses. Neuroimage 57, 22–36.

Schmid, M.C., Mrowka, S.W., Turchi, J., Saunders, R.C., Wilke, M., Peters, A.J., Ye, F.Q., Leopold, D.A., 2010. Blindsight depends on the lateral geniculate nucleus. Nature 466, 373–377.

Schmuel, A., Yacoub, E., Pfeuffer, J., Van de Moortele, P.-F., Adriany, G., Hu, X., Ugurbil, K., 2002. Sustained negative BOLD, blood flow and oxygen consumption response and its coupling to the positive response in the human brain. Neuron 36, 1195–1210.

Schoenfeld, M.A., Noesselt, T., Poggel, D., Tempelmann, C., Hopf, J.M., Woldorff, M.G., Heinze, H.J., Hillyard, S.A., 2002. Analysis of pathways mediating preserved vision after striate cortex lesions. Ann. Neurol. 52, 814–824.

Shmuel, A., Leopold, D.A., 2008. Neuronal correlates of spontaneous fluctuations in fMRI signals in monkey visual cortex: implications for functional connectivity at rest. Hum. Brain Mapp. 29, 751–761.

Sillito, A., Cudeiro, J., Jones, H., 2006. Always returning: feedback and sensory processing in visual cortex and thalamus. Trends Neurosci. 29, 307–316.

Sincich, L.C., Park, K.F., Wohlgemuth, M.J., Horton, J.C., 2004. Bypassing V1: a direct geniculate input to area MT. Nat. Neurosci. 7, 1123–1128.

Small, D.M., Zald, D.H., Jones-Gotman, M., Zatorre, R.J., Pardo, J.V., M.F.S.a.P., 1999. Human cortical gustatory areas: a review of functional neuroimaging data. Neuroreport 10, 7–14.

Stepniewska, I., Qi, H.X., Kaas, J.H., 1999. Do superior colliculus projection zones in the inferior pulvinar project to MT in primates? Eur. J. Neurosci. 11, 469–480.

Sun, F., 2004. Measuring interregional functional connectivity using coherence and partial coherence analyses of fMRI data. Neuroimage 21, 647–658.

Sun, F.T., Miller, L.M., D'Esposito, M., 2005. Measuring temporal dynamics of functional networks using phase spectrum of fMRI data. Neuroimage 28, 227–237.

Talairach, J., Tournoux, P., 1988. Co-planar Stereotaxic Axis of the Human Brain.

Tootell, R.B., Reppas, J.B., Kwong, K.K., Malach, R., Born, R.T., Brady, T.J., Rosen, B.R., Belliveau, J.W., 1995. Functional analysis of human MT and related visual cortical areas using magnetic resonance imaging. J. Neurosci. 15, 3215–3230.

Ungerleider, L.G., Desimone, R., Galkin, T.W., Mishkin, M., 1984. Subcortical projections of area MT in the macaque. J. Comp. Neurol. 223, 368–386.

Valdes-Sosa, P.A., Roebroeck, A., Daunizeau, J., Friston, K., 2011. Effective connectivity: influence, causality and biophysical modeling. Neuroimage 58, 339–361.

Wan, X., Nakatani, H., Ueno, K., Asamizuya, T., Cheng, K., Tanaka, K., 2011. The neural basis of intuitive best next-move generation in board game experts. Science 331, 341–346.

Warner, C.E., Goldshmit, Y., Bourne, J.A., 2010. Retinal afferents synapse with relay cells targeting the middle temporal area in the pulvinar and lateral geniculate nuclei. Front. Neuroanat. 4, 8.

Whalen, P.J., Rauch, S.L., Etcoff, N.L., McInerney, S.C., Lee, M.B., Jenike, M.A., 1998. Masked presentations of emotional facial expressions modulate amygdala activity without explicit knowledge. J. Neurosci. 18, 411–418.

Zeki, S., 1995. The motion vision of the blind. Neuroimage 2, 231–235.

Zeki, S., Ffytche, D.H., 1998. The Riddoch syndrome: insights into the neurobiology of conscious vision. Brain 121 (Pt 1), 25–45.